

Conformational Behavior of Serine: An Experimental Matrix-Isolation FT-IR and Theoretical DFT(B3LYP)/6-31++G** Study

Bert Lambie, Riet Ramaekers, and Guido Maes*

Department of Chemistry, University of Leuven, Celestijnenlaan 200 F, B-3001 Leuven, Belgium

Received: June 28, 2004; In Final Form: September 1, 2004

The conformational equilibria of neutral serine are studied by experimental matrix-isolation Fourier transform infrared spectroscopy in combination with density functional theory (DFT) calculations. The geometries and energies of the low-energy conformers of serine were optimized using the DFT(B3LYP)/6-31++G** method. In addition, we calculated the infrared frequencies and intensities of the most stable conformers in order to assist in the assignment of the vibrational bands in the experimental spectrum. The calculated relative energies suggest that four conformers are sufficiently stable to appear in the gas phase and all could be distinguished in the experimental matrix infrared spectra. We also calculated theoretical rotamerization constants and compared these with experimental determined constants. For the equilibria SER2/SER1 and SER3/SER1, a deviation between the experimental rotamerization constant and the theoretical constant was found. A relatively strong intramolecular H-bond in conformers SER2 and SER3 is at the origin of this discrepancy.

Introduction

The conformational behavior of neutral amino acids and their vibrational characteristics are of particular interest for several reasons. The intrinsic conformational properties and energies determine to a large extent the functional specificity of proteins and polypeptides.¹ Furthermore, one can apply the data obtained by detailed studies in the search for the origin and signs of life in interstellar space.² The performance of the present theoretical methods can be examined by comparison of the calculated data with the experimental results. Consequently, this study can contribute to the development of better or more reliable computational methods, both semiempirical and ab initio.³

Serine is an α -amino acid with a hydroxyl group in the side chain. This amino acid is required for the metabolism of fat, tissue growth, and the immune system as it assists in the production of immunoglobulins and antibodies. It is also an important constituent of brain proteins and nerve coverings. Adequate amounts of serine can be found in meat and dairy products, wheat gluten, and peanuts, as well as in soy products.⁴

Since most amino acids possess a low symmetry, the multiple internal rotational degrees of freedom lead to a large number of different low energy conformers on the potential energy surface. Several research groups have reported theoretical studies on the conformational space of neutral serine. However, most of these computations have only considered a subset of conformers or were achieved at a rather poor level of theory.^{5–7} The most complete theoretical investigation of the potential energy surface has been performed by Gronert and O'Hair.⁸ To identify all minima on the potential energy surface, the authors initially surveyed a starting set of 324 conformers based on all possible combinations of single-bond rotamers (Figure 1) at the semiempirical AM1 level. Then, 73 unique conformers from the AM1 optimization were optimized at the HF/6-31G* level. The 51 conformers with relative energy differences smaller than 50 kJ/mol were finally subjected to single point calculations

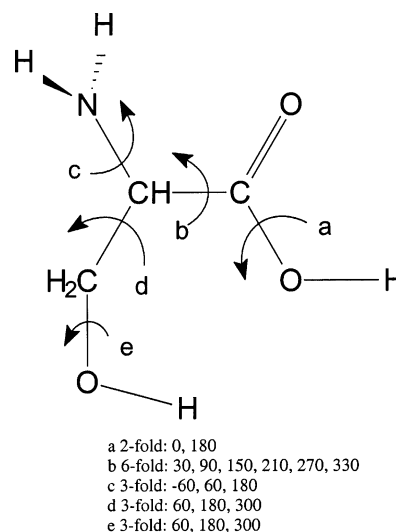


Figure 1. Possible internal rotations (deg) in serine.

on the MP2/6-31+G* level. Recent studies have treated other theoretical parameters of serine such as proton affinities, intrinsic basicities, and vibrational frequencies.^{9,10}

Experimental studies on neutral amino acids are rather scarce, mainly because of the low thermal stability and low vapor pressure of these compounds. Since most amino acids decompose before melting, it is extremely difficult to obtain a concentration in the gas phase sufficient for infrared studies. Matrix-isolation is a powerful tool to simulate the gas phase. Since the molecules are isolated in a rigid cage of inert atoms, such as Ar, Kr, and so forth, environmental interactions are for a large part excluded. Moreover, the rigid matrix prevents rotation of the molecules, and no rotational fine structure complicates the spectrum. Until now and to the best of our knowledge, only the amino acids glycine, alanine, proline, and valine have been studied experimentally using the matrix-isolation technique.^{11–15}

In this work, we investigate the conformational behavior of neutral serine isolated in low-temperature Ar matrices. Earlier

* To whom correspondence should be addressed. Phone: 0032 16 32 74 50. Fax: 0032 16 32 79 92. E-mail: guido.maes@chem.kuleuven.ac.be.

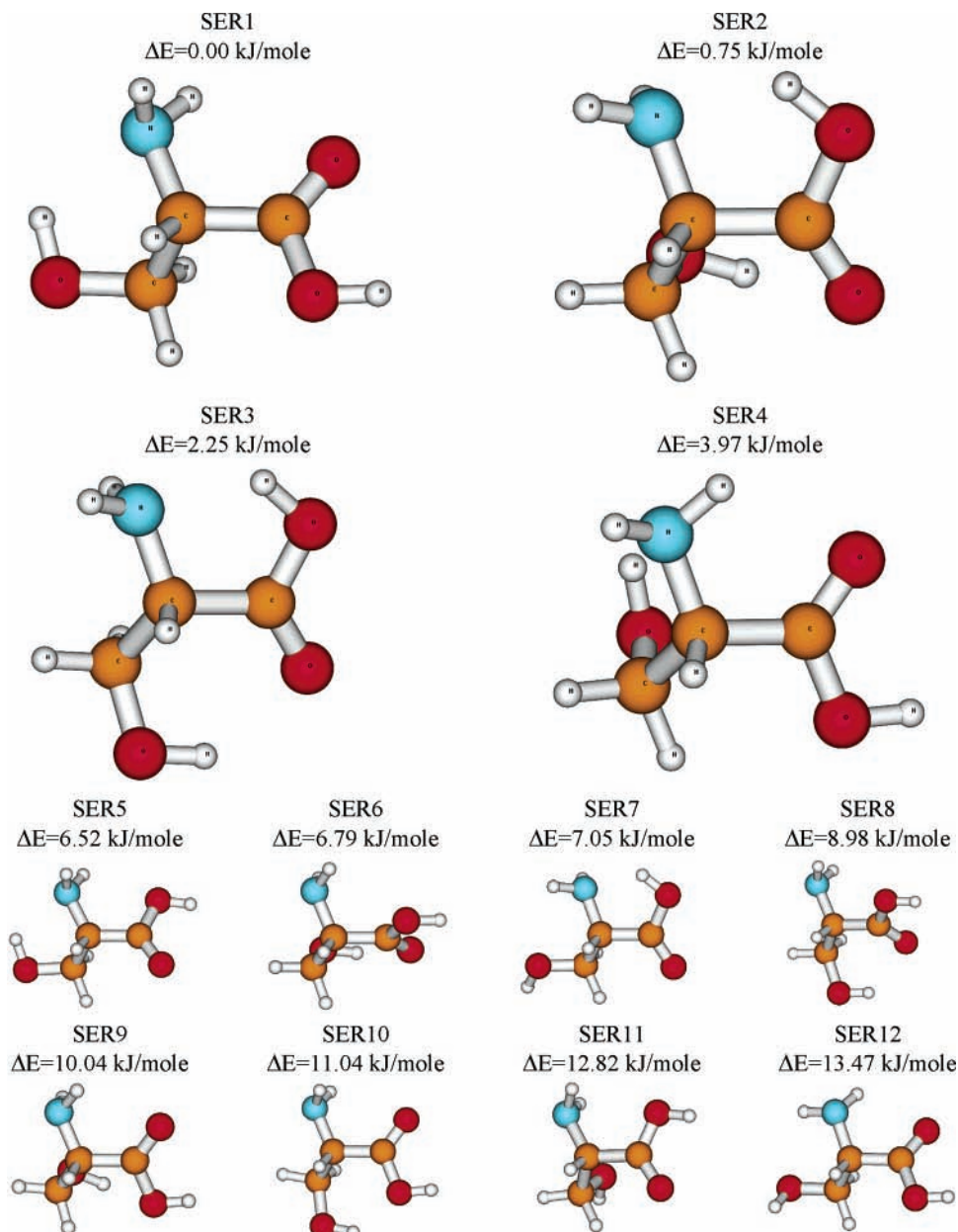


Figure 2. Optimal geometries and relative energies (DFT(B3LYP)/6-31++G**) of the 12 most stable conformers of serine.

attempts to evaporate the compound were unsuccessful due to its partial decomposition. By optimization of the dimensions and the position of the sublimation cell, it became possible to obtain IR matrix spectra without traces of the decomposition products CO_2 and H_2O . The experimental infrared spectral characteristics of serine are evaluated using theoretically calculated data, and theoretical rotamerization constants are compared with experimental values. In addition, the reliability of the theoretical methods is evaluated.

Theoretical Methods

The geometries, the energies and the vibrational frequencies of the serine conformers were calculated using the density functional theory (DFT) method. The calculations were performed with Becke's nonlocal three-parameter hybrid functional in combination with the Lee, Yang, and Parr correlation functional (B3LYP).^{16,17} It has been shown before that the B3LYP density functional method performs very well in studies on the conformational behavior of amino acids,^{10–12} since the

results are in very good agreement with other correlated methods such as MP2 at a lower computational cost. For the molecular orbital expansion, we used a split valence double- ζ basis set, with extra polarization and diffuse functions (6-31++G**). The use of a basis set with sufficient diffuseness and angular flexibility is indispensable to obtain reliable results for H-bonded amino acids which is the interest of our future research.¹⁸ All quantum chemical calculations were performed using the PQS Ab Initio Program Package version 2.5.¹⁹ We also used the SQM add-on module to scale force constants in order to produce a scaled quantum mechanical force field.²⁰ The latter is necessary to correct for deficiencies in the calculated (harmonic) force constants, giving a better fit to experimentally observed vibrational frequencies and infrared intensities.²¹

Experimental Details

The cryogenic equipment used in the matrix-isolation experiments has been described in detail elsewhere.^{22,23} Serine was evaporated in a homemade mini furnace positioned close to the

TABLE 1: DFT(B3LYP)/6-31++G Energies, Zero-Point Vibrational Energies (ZPE), Relative Stabilities (ΔE) and Dipole Moments of the Four Most Stable Serine Conformers (See Figure 2)**

	SER1	SER2	SER3	SER4
energy (au)	-398.996371646	-398.996476857	-398.996112778	-398.994806913
ZPE ^a (au)	0.110153222	0.110544308	0.110751444	0.110102211
total energy ^b (au)	-398.8862184	-398.8859325	-398.8853613	-398.8847047
ΔE^c (kJ mol ⁻¹)	0.00	0.75	2.25	3.97
dipole moment (D)	2.13	4.30	5.24	3.06

^a ZPE values scaled with the uniform scaling factor 0.97. ^b ZPE corrected energies (au). ^c Energy difference between the different conformers relative to the most stable conformer SER1.

cold CsI window inside the cryostat. This vapor was mixed with a large excess of Ar and deposited on the cold window in order to obtain a rigid matrix. The optimal sublimation temperature of monomeric serine was found to be 353 K. This temperature was high enough to yield matrices with sufficient concentration of serine but still sufficiently low to prevent product decomposition. The infrared spectra of the compound were obtained by Fourier transformation of 128 interferograms scanned on a Bruker IFS66 instrument at a resolution of 1 cm⁻¹. To check whether any decomposition of the sample has occurred, an infrared spectrum of the solid compound was recorded before and after heating in the furnace.

The studied compound (L-serine, $\geq 99.5\%$) was obtained from Fluka. High purity argon gas (N60 = 99.99990%) was purchased from Air Liquide.

Results and Discussion

The 12 most stable conformers of serine were selected from the work of Gronert and O'Hair,⁸ and these were used as a starting point for the geometry optimizations on the DFT-(B3LYP)/6-31++G** level in this work. Figure 2 illustrates the optimal geometries as well as the calculated energy differences relative to the most stable conformer 1.

Only the four most stable conformers with a relative energy difference smaller than 5 kJ mol⁻¹ are further analyzed and discussed. As a matter of fact, in earlier studies on comparable compounds it has been demonstrated that the abundance of conformers with a larger relative energy difference is too small, which makes identification of these forms in the experimental spectrum difficult or even impossible.¹⁵

Table 1 lists the obtained theoretical parameters of the four most stable serine conformers, further denoted as SER1, SER2, SER3, and SER4.

The formula $\Delta H^\circ - T\Delta S^\circ = \Delta G^\circ = -RT \ln K_r$ can be used to estimate the theoretical rotamerization constant, K_r , for the different rotameric equilibria. For SER5 with a ΔG° value of 5.18 kJ mol⁻¹ relative to SER1, the theoretical K_r (SER5/SER1) is 0.16 at the sublimation temperature. Taking into account also the three other equilibria, SER2/SER1 with theoretical $K_r = 0.55$, SER3/SER1 with theoretical $K_r = 0.22$, and SER4/SER1 with theoretical $K_r = 0.19$, we can conclude that SER5 will only be present for about 6% in the gas phase and thus in the experimental Ar-matrix. The experimental identification of SER5 will therefore be extremely difficult. For this reason, we have decided to limit the further analysis to the four most stable forms.

Even though the two most stable conformers, SER1 and SER2, are energetically comparable ($\Delta E = 0.75$ kJ mol⁻¹), their structures are quite different. SER1 has a rather weak intramolecular hydrogen bond between one of the H atoms of the amino group and the O atom of the carbonyl group and another, also weak intramolecular hydrogen bond between the O-H group of the side chain and the N atom of the amino group. On

the contrary, in SER2 a strong intramolecular H-bond exists between the O-H group of the carboxyl group and the N atom of the amino group and a weaker one between one of the amino H atoms and the O atom of the side chain. In this form, the O-H group of the side chain is pointed toward the oxygen of the carbonyl group. The structure of SER3 ($\Delta E = 2.25$ kJ mol⁻¹) is comparable with SER2, but any attraction between the amino H atom and the O atom of the side chain is absent because the side chain is rotated, and therefore, the H-bond between the O-H group of the side chain and the carbonyl O atom becomes much stronger. The structure of SER4 ($\Delta E = 3.97$ kJ mol⁻¹) is comparable with that of SER1, the only difference being the fact that the rotated side chain gives rise to a somewhat different orientation of the intramolecular H-bonds.

The presence of H-bonds of different natures in the four conformers allows to distinguish between the IR spectra of the four most stable forms. Figure 3a illustrates the sum of the theoretically computed IR spectra of the four most stable conformers of serine. The abundance of the four forms in this spectrum reflects the relative energy differences between the conformers. Figure 3b shows the experimental matrix-isolation FT-IR spectrum of serine. Very small amounts of water are observable in this spectrum. However, it is essentially free water, which does not perturb the product spectrum. The $\nu(\text{OH})$ region around 3500 cm⁻¹ is quite different for the computed and experimental spectra, which is due to different H-bonding, and the different broadening effects are not taken into account in the theoretical spectrum. The observed frequencies and intensities are analyzed by comparison with the predicted theoretical spectra at the DFT(B3LYP)/6-31++G** level for the four most stable serine conformers. The results are listed in Table 2. To correct for the various systematic deficiencies in the theoretical approach, i.e., the neglect of the vibrational anharmonicity, the use of a finite basis set, and the incomplete account for electron correlation, the force constants are scaled. The SQM package,²⁰ implemented in the PQS program,¹⁹ was used for this purpose. The scaling of force constants has been demonstrated to yield much better results than the scaling of frequencies.²¹ Additionally, scaling the force constant matrix also affects the calculated intensities, which are unaffected if only the frequencies are scaled. This leads to a better agreement with experimental intensities too. We used the already available experimental and theoretical (B3LYP/6-31++G**) frequencies of different conformers of glycine and alanine^{11,15} to derive a set of scaling factors for various primitive stretching, bending, and torsional force constants. Table 3 lists these optimal scaling factors for amino acids, and these scaling factors are further used in this work.

The spectral region between 3650 and 2800 cm⁻¹ of the experimental infrared spectrum is shown in more detail in Figure 4, since this region can be used to distinguish between the four different conformers, in particular the O-H stretching bands.

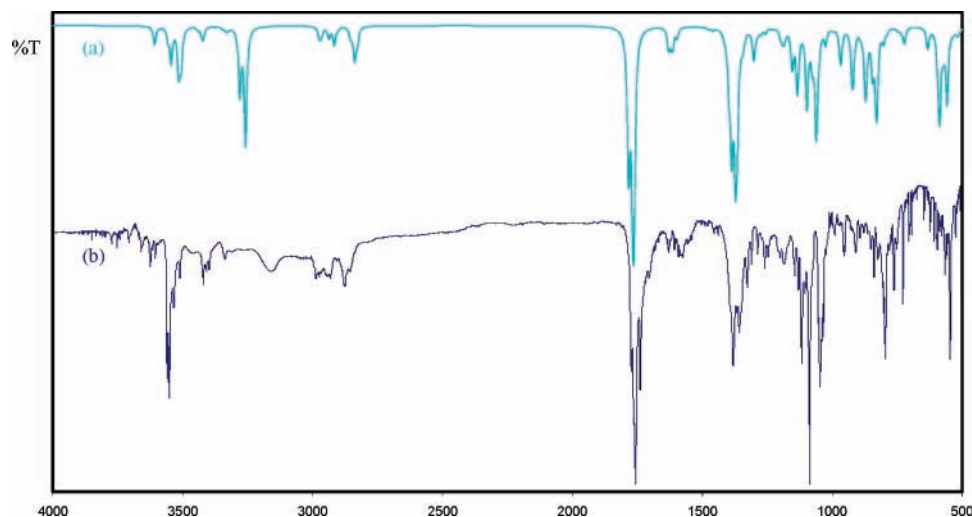


Figure 3. (a) Theoretical (DFT(B3LYP)/6-31++G**) vibrational spectrum of the four most stable conformers of serine, scaled to their relative abundance. (b) Experimental matrix FT-IR spectrum of serine in Ar at 15 K (sublimation temperature: 353 K).

Because the O–H group of the main skeleton in SER2 and SER3 is strongly H-bonded with the amino N atom, the $\nu(\text{OH})$ mode of this group is strongly red shifted, and the intensity is larger than that of the $\nu(\text{OH})$ mode in SER1 and SER4. By comparison with the calculated frequencies, the intense band observed around 3556 cm^{-1} can be assigned to the free O–H stretching mode of SER1. The high frequency shoulder on this band is most probably due to the same vibrational mode in SER4. The broad band (typical for H-bonds) observed at 3169 cm^{-1} in the experimental spectrum is the H-bonded OH stretching band originating from the O–H group in SER2, while the high frequency shoulder is most probably due to the same band in SER3.

The O–H group of the side chain of serine is also weakly H-bonded to an electronegative atom (N or O). The theoretically calculated H-bond distances reflect the strength of the H-bonds. The H-bond is the weakest in SER2, with a H-bond length of 2.83 \AA . The frequency of the $\nu(\text{OH})$ stretching vibration is calculated at 3608 cm^{-1} and can easily be assigned to the experimental band at 3610 cm^{-1} . The H-bond lengths in SER1 and SER4 are comparable, i.e., 2.24 and 2.27 \AA , respectively. The slightly stronger H-bonds compared to SER2 are manifested by a small red shift to 3515 and 3517 cm^{-1} , for SER1 and SER4, respectively. In the experimental spectrum, these modes are simultaneously assigned to the band at 3540 cm^{-1} . In SER3, the H-bond distance is decreased to 2.04 \AA , in accordance with a theoretically smaller frequency, i.e., 3506 cm^{-1} , which corresponds to the experimental value of 3516 cm^{-1} .

The stretching vibrations of the amino group are not very useful to distinguish one conformer from the others. The predicted frequency values for the four forms are very close to each other, and the intensities of these bands are rather small. The asymmetric $\nu^{\text{as}}(\text{NH}_2)$ frequencies of the four conformers, which are all predicted in the same region at around 3430 cm^{-1} , can all together be assigned to the group of bands observed around 3426 cm^{-1} . In the experimental spectrum, the $\nu^{\text{s}}(\text{NH}_2)$ frequencies are predicted to be about 100 cm^{-1} smaller than the asymmetric ones and can be assigned to the band observed at around 3344 cm^{-1} .

The C–H stretching vibrations are situated below 3000 cm^{-1} . The assignments of these bands are listed in Table 2. Since the C–H stretching vibration of the C–H group in the main part of serine is predicted to have a very small intensity, the assignment of this band is somewhat tentative (Table 2).

The irregular band shape of the intense $\nu(\text{C}=\text{O})$ band in the experimental spectrum also clearly demonstrates the presence of different conformers. The carbonyl group in SER1, which is weakly hydrogen bonded to both amino H atoms, is predicted at 1763 cm^{-1} . The same mode in SER2, weakly hydrogen bonded to the hydroxyl group of the side chain, is predicted 25 cm^{-1} higher at 1788 cm^{-1} with about the same high intensity. For SER3 and SER4, the carbonyl stretching vibration is predicted around 1770 cm^{-1} , i.e., between the values for the two former conformations. The experiments reflect the predictions very well in this region. The intense $\nu(\text{C}=\text{O})$ band at 1773 cm^{-1} is assigned to SER1, the $\nu(\text{C}=\text{O})$ band at 1788 cm^{-1} originates from SER2, and the high frequency shoulder of the band at 1773 cm^{-1} must originate from SER3 and SER4.

Around 1400 cm^{-1} in the experimental spectrum, a rather broad band is observed. This band is due to the bending vibration of all hydrogen-bonded hydroxyl groups in the main skeleton as well as in the side chain of the different conformations. A little blue shifting and broadening is noticed compared to the bending vibration in the non-hydrogen-bonded hydroxyl groups.

The intense absorption at 1105 cm^{-1} in the experimental spectrum is probably due to a combination of the N–C and the C–O stretching vibrations as well as the O–H bending vibration in the main skeleton of SER1.

The C–O stretching mode in the side chain of SER1 is also predicted to be intense and is found experimentally at 1066 cm^{-1} . Two low frequency shoulders near this band (± 1061 and 1053 cm^{-1}) come from the same mode of SER3 and SER4, predicted at 1064 and 1054 cm^{-1} , respectively. The same mode is predicted about 100 cm^{-1} lower (967 cm^{-1}) and is observed at 973 cm^{-1} for SER2.

The out-of-plane NH_2 mode of the different conformations is predicted to be intense. The relative broad band at 816 cm^{-1} with low and high frequency shoulders can be assigned to this mode.

For SER1, the combination band of $\gamma(\text{CH}_2)$ and $\gamma(\text{OH})$ is predicted at 558 cm^{-1} with an intensity of $131\text{ km}\cdot\text{mol}^{-1}$. This mode is assigned in the experimental spectrum to the intense band at 568 cm^{-1} . For SER4, the combination of several modes, $\gamma(\text{CH}_2)$, $\delta(\text{C}=\text{O})$, $\delta(\text{C}=\text{O})$ and $\gamma(\text{OH})$, also gives rise to a band at 558 cm^{-1} according to the calculations, albeit with a much

TABLE 2: Experimental and Calculated (DFT(B3LYP)/6-31++G) IR Frequencies (cm⁻¹) and Intensities (km mol⁻¹) of the Four Most Stable Conformers of Serine (See Figure 2)**

obsd ^a ν	calculated								PED ^c
	SER1		SER2		SER3		SER4		
	ν	I_{calc}^b	ν	I_{calc}^b	ν	I_{calc}^b	ν	I_{calc}^b	
3610			3608	44					$\nu(\text{OH})_{\text{sc}}$
3556	3544	65					3556	80	$\nu(\text{OH})_{\text{bb}}$
3540	3515	69					3517	58	$\nu(\text{OH})_{\text{sc}}$
3516					3506	138			$\nu(\text{OH})_{\text{sc}}$
3426	3420	12			3426	13			$\nu^{\text{as}}(\text{NH}_2)$
3414			3424	17					$\nu^{\text{as}}(\text{NH}_2)$
3344	3334	6							$\nu^{\text{s}}(\text{NH}_2)$
3317			3326	7					$\nu^{\text{s}}(\text{NH}_2)$
3169			3258	283	3280	259			$\nu(\text{OH})_{\text{bb}}$
2995	2973	19							$\nu^{\text{as}}(\text{CH}_2) + \nu^{\text{s}}(\text{CH}_2)$
2983			2965	18					$\nu^{\text{as}}(\text{CH}_2)$
2940	2936	7							$\nu(\text{CH})$
					2938	30			$\nu^{\text{as}}(\text{CH}_2) + \nu^{\text{s}}(\text{CH}_2)$
2915					2915	10			$\nu(\text{CH})$
2885			2917	39					$\nu^{\text{s}}(\text{CH}_2)$
2864	2838	54					2854	76	$\nu^{\text{s}}(\text{CH}_2) + \nu^{\text{as}}(\text{CH}_2)$
2845					2828	60			$\nu^{\text{as}}(\text{CH}_2) + \nu^{\text{s}}(\text{CH}_2)$
1788			1784	324					$\nu(\text{C}=\text{O})$
1773	1763	306			1770	304	1767	295	$\nu(\text{C}=\text{O})$
1646	1630	38							$\delta(\text{NH}_2)$
1624					1620	41			$\delta(\text{NH}_2)$
1608			1614	40					$\delta(\text{NH}_2)$
1590							1597	73	$\delta(\text{NH}_2)$
1476	1479	2			1477	2			$\delta(\text{CH}_2)$
1457			1460	7					$\delta(\text{CH}_2)$
1409					1414	17	1403	40	$\delta(\text{OH})_{\text{sc}} + \rho(\text{CH}_2)$
1399	1397	69							$\delta(\text{OH})_{\text{sc}} + \rho(\text{CH}_2)$
1384	1393	10							$\delta(\text{CH})$
			1387	246					$\delta(\text{OH})_{\text{bb}} + \rho(\text{CH}_2)$
							1386	38	$\delta(\text{OH})_{\text{sc}} + \rho(\text{CH}_2)$
1374					1373	472			$\delta(\text{OH})_{\text{bb}} + \nu(\text{C}-\text{O})_{\text{bb}}$
			1366	194					$\rho(\text{CH}_2) + \delta(\text{OH})_{\text{bb}}$
1367			1363	6					$\rho(\text{CH}_2)$
1344			1346	18					$\delta(\text{OH})_{\text{sc}}$
					1343	27			$\rho(\text{CH}_2) + \delta(\text{OH})_{\text{sc}}$
1328	1338	3							$\rho(\text{CH}_2) + \delta(\text{OH})_{\text{sc}}$
1305	1302	57							$\delta(\text{OH})_{\text{bb}} + \nu(\text{C}-\text{O})_{\text{bb}}$
1289							1291	37	$\delta(\text{OH})_{\text{bb}} + \nu(\text{C}-\text{O})_{\text{bb}}$
					1282	6			$\delta(\text{C}-\text{C})_{\text{sc}} + \gamma(\text{CH})$
1278			1274	10					$\gamma(\text{CH}) + \delta(\text{CH})$
1265	1257	10							$\rho(\text{CH}_2) + \delta(\text{OH})_{\text{sc}} + \rho(\text{NH}_2)$
1227	1228	7							$\delta(\text{OH})_{\text{bb}} + \delta(\text{CH}) + \gamma(\text{CH})$
1204			1200	14					$\delta(\text{OH})_{\text{sc}} + \nu(\text{N}-\text{C})$
					1197	6			$\nu(\text{C}-\text{O})_{\text{bb}} + \delta(\text{OH})_{\text{bb}} + \nu(\text{C}-\text{C})_{\text{bb}}$
1200					1191	22			$\delta(\text{OH})_{\text{sc}} + \rho(\text{CH}_2)$
1186			1187	15					$\nu(\text{C}-\text{O})_{\text{bb}} + \delta(\text{OH})_{\text{bb}} + \nu(\text{C}-\text{C})_{\text{bb}}$
							1183	47	$\rho(\text{CH}_2) + \delta(\text{OH})_{\text{sc}} + \rho(\text{NH}_2)$
1163					1157	8			$\rho(\text{NH}_2)$
1150	1154	65							$\delta(\text{OH})_{\text{ss}} + \tau(\text{CH}_2) + \rho(\text{NH}_2)$
			1149	5					$\delta(\text{OH})_{\text{sc}} + \rho(\text{NH}_2)$
1136	1135	80							$\nu(\text{C}-\text{O})_{\text{bb}} + \delta(\text{OH})_{\text{bb}} + \nu(\text{N}-\text{C})$
1124							1132	174	$\nu(\text{C}-\text{O})_{\text{bb}} + \delta(\text{OH})_{\text{bb}}$
1105	1098	130							$\nu(\text{N}-\text{C}) + \nu(\text{C}-\text{O})_{\text{bb}} + \delta(\text{OH})_{\text{bb}}$
1093					1086	9	1095	68	$\nu(\text{N}-\text{C}) + \nu(\text{C}-\text{C})_{\text{sc}}$
1073			1077	68					$\nu(\text{C}-\text{O})_{\text{sc}} + \nu(\text{N}-\text{C}) + \nu(\text{C}-\text{C})_{\text{sc}}$
1066	1061	150							$\nu(\text{C}-\text{O})_{\text{sc}}$
1061					1064	105			$\nu(\text{C}-\text{O})_{\text{sc}}$
1053							1054	92	$\nu(\text{C}-\text{O})_{\text{sc}}$
			1053	15					$\nu(\text{C}-\text{O})_{\text{sc}} + \gamma(\text{NH}_2) + \nu(\text{N}-\text{C})$
1029					1026	58			$\nu(\text{C}-\text{C})_{\text{sc}} + \nu(\text{C}-\text{O})_{\text{bb}} + \gamma(\text{NH}_2)$
993	998	2							$\nu(\text{C}-\text{C})_{\text{sc}} + \gamma(\text{NH}_2)$
973			967	82					$\nu(\text{C}-\text{O})_{\text{sc}}$
971					973	17			$\nu(\text{N}-\text{C})$
931	924	67							$\nu(\text{C}-\text{C})_{\text{bb}} + \gamma(\text{NH}_2)$
914			919	86					$\gamma(\text{NH}_2)$
885							891	29	$\nu(\text{C}-\text{C})_{\text{sc}} + \nu(\text{C}-\text{O})_{\text{sc}}$
873			874	62					$\gamma(\text{OH})_{\text{bb}}$
870	872	41							$\nu(\text{C}-\text{C})_{\text{sc}}$
					870	86			$\gamma(\text{OH})_{\text{bb}}$
860							866	85	$\gamma(\text{NH}_2)$

TABLE 2: (Continued)

obsd ^a ν	calculated								
	SER1		SER2		SER3		SER4		PED ^c
	ν	I_{calc}^b	ν	I_{calc}^b	ν	I_{calc}^b	ν	I_{calc}^b	
846			845	96					$\nu(\text{N}-\text{C}) + \gamma(\text{OH})_{\text{bb}} + \nu(\text{C}-\text{C})_{\text{sc}}$
828					832	142			$\gamma(\text{NH}_2) + \gamma(\text{OH})_{\text{bb}}$
816	828	115							$\gamma(\text{NH}_2) + \nu(\text{N}-\text{C}) + \nu(\text{C}-\text{C})_{\text{bb}}$
808			805	7					$\gamma(\text{OH})_{\text{bb}}$
800							802	77	$\gamma(\text{OH})_{\text{bb}} + \gamma(\text{NH}_2)$
785					789	15			$\nu(\text{C}-\text{C})_{\text{bb}} + \nu(\text{C}-\text{O})_{\text{bb}}$
749			749	7					$\nu(\text{C}-\text{C})_{\text{bb}} + \delta(\text{C}=\text{O}) + \nu(\text{C}-\text{O})_{\text{bb}}$
736							735	31	$\nu(\text{C}-\text{C})_{\text{bb}} + \nu(\text{C}-\text{C})_{\text{sc}} + \nu(\text{C}-\text{O})_{\text{bb}}$
723					725	7			$\delta(\text{C}=\text{O})$
	722	28							$\gamma(\text{OH})_{\text{bb}} + \nu(\text{C}-\text{C})_{\text{sc}}$
643	633	19							$\delta(\text{C}=\text{O}) + \nu(\text{C}-\text{O})_{\text{bb}}$
592					593	87			$\gamma(\text{CH}_2) + \gamma(\text{OH})_{\text{sc}}$
589							589	161	$\gamma(\text{OH})_{\text{sc}} + \gamma(\text{CH}_2) + \delta(\text{C}-\text{C})_{\text{bb}}$
	586	121							$\gamma(\text{OH})_{\text{bb}} + \gamma(\text{C}=\text{O})$
585			584	6					$\delta(\text{C}-\text{C})_{\text{bb}} + \delta(\text{C}-\text{O})_{\text{sc}}$
576					572	56			$\gamma(\text{OH})_{\text{sc}} + \delta(\text{C}-\text{O})_{\text{bb}}$
568	558	131							$\gamma(\text{CH}_2) + \gamma(\text{OH})_{\text{sc}}$
560							558	24	$\gamma(\text{CH}_2) + \delta(\text{C}-\text{O})_{\text{bb}} + \delta(\text{C}=\text{O}) + \gamma(\text{OH})_{\text{sc}}$
532			536	7					$\delta(\text{C}=\text{O}) + \nu(\text{C}-\text{C})_{\text{bb}}$
526					529	5			$\delta(\text{C}=\text{O}) + \nu(\text{C}-\text{C})_{\text{bb}}$
520							520	29	$\gamma(\text{OH})_{\text{bb}}$
513	515	9							$\delta(\text{C}-\text{O})_{\text{bb}}$
507			507	3					$\delta(\text{C}=\text{O}) + \delta(\text{C}-\text{O})_{\text{bb}}$

^a Ar matrix deposited at 15 K. ^b Calculated intensities in $\text{km}\cdot\text{mol}^{-1}$. ^c Potential energy distributions, only contributions $\geq 10\%$ are listed. Subscripts: sc, side chain; bb, common part of amino acids.

TABLE 3: Optimized Force Constant Scaling Factors for Amino Acids Derived from Experimental and Theoretical (DFT(B3LYP)/6-31++G**) Data of Glycine and Alanine^a

vibrational mode	scaling factor
stretch X-X	0.9491
stretch C-H	0.9057
stretch N-H	0.9025
stretch O-H	0.8949
bend X-X-X	0.9377
bend X-X-H	0.9497
bend H-C-H	0.9391
bend H-N-H	0.9473
torsion X-X-X-X	1.0402
torsion H-X-X-X	0.9532
torsion H-X-X-H	0.9712

^a Data taken from refs 11 and 15.

smaller intensity ($24 \text{ km}\cdot\text{mol}^{-1}$). The low-frequency shoulder (560 cm^{-1}) of the former band of SER1 is assigned to this band of SER4.

The combination of experimental and theoretical intensities of some characteristic bands of SER2 with some bands of SER1 allows us to estimate the position of the experimental conformational equilibrium SER2/SER1. The value of the rotamerization constant K_r (denoted as “experimental” constant) is calculated using the procedure earlier described by Nowak et al.:²⁵⁻²⁷

$$K_r = \frac{[\text{SER2}]}{[\text{SER1}]} = \frac{I_{\text{SER2}}/A_{\text{SER2}}}{I_{\text{SER1}}/A_{\text{SER1}}}$$

with I_i the experimental and A_i the theoretically predicted intensity. The same procedure can be applied to the other equilibria, i.e., SER3/SER1 and SER4/SER1.

Because of the similar structure of the four conformers, it is rather difficult to select from the experimental spectrum completely separated bands of the different conformers which do not overlap with bands from other conformers. Table 4 lists a selection of possible candidate bands for the four conformers

and the experimental K_r values for the first two conformational equilibria, i.e., SER2/SER1 and SER3/SER1. Unfortunately, it was not possible to select any experimental vibration band of SER4 which could be integrated accurately.

The theoretical rotamerization constant $K_r(\text{SER2/SER1}) = 0.55$, calculated from the free energy difference between these two conformations, deviates slightly from the experimentally obtained K_r value ($=0.31 \pm 0.10$) for this equilibrium. The reason for this discrepancy is the presence of different intramolecular H-bonds in SER1 and SER2. It is however not possible to calculate the ΔS value for one individual intramolecular H-bond, which was clearly possible for glycine and alanine.^{15,24} For the second equilibrium between SER3 and SER1, the theoretical K_r value was calculated to be 0.22. The experimentally obtained K_r value is, as expected, smaller ($K_r = 0.05 \pm 0.01$). The different intramolecular H-bonds (i.e., different nature of proton donor and/or acceptor or different orientation of the bond), and therefore the different contribution of the entropy term in the free energy equation, are again the main reason for this discrepancy.

By comparing the observed and the theoretical frequencies, the “new” scaling procedure based on the force constants used in this work can be evaluated. The mean frequency deviation $|\Delta\nu| = |\nu_{\text{exp}} - \nu_{\text{theor}}|$ is 7.56 cm^{-1} , taking into account all assigned vibrational modes of the four conformers. The optimal scaling factor for the O-H stretching vibrations is calculated as 0.8949 for six conformers of glycine and alanine (Table 3). Because only two of these six conformers have a strong intramolecular H-bond involving the O-H group, this scaling factor is insufficient to completely account for the anharmonicity in strongly H-bonded O-H groups. The large anharmonicity of the strongly H-bonded O-H groups in SER2 and SER3 explains why we observe a large deviation between the experimental and the theoretical frequency values for this vibrational mode. When the latter two frequencies are ignored in the calculation of the mean frequency deviation, the final $|\Delta\nu| = |\nu_{\text{exp}} - \nu_{\text{theor}}|$ decreases to 5.56 cm^{-1} . As expected, the

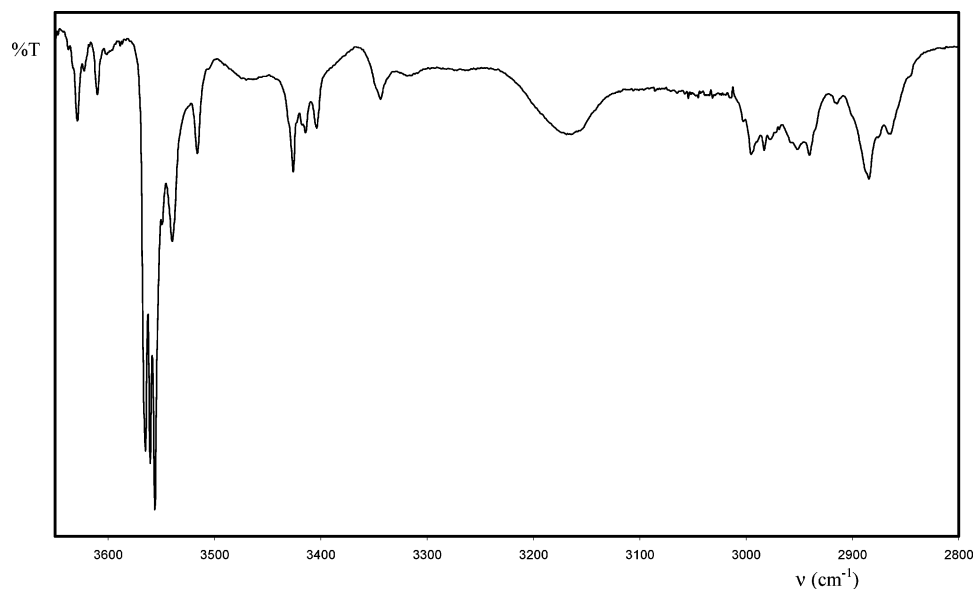


Figure 4. Enlarged high-frequency region (3650–2800 cm^{-1}) of the experimental matrix FT-IR spectrum of serine in Ar at 15 K (sublimation temperature: 353 K).

TABLE 4: Estimation of the Experimental Rotamerization Constants for Serine in Ar (Sublimation Temperature 353 K)

			$K_r[\text{SER2/SER1}]$						
			SER1 ν (cm^{-1}):	3344	1646	1399	1265	1136	1105
			SER1 I_{exp} :	0.169	0.836	1.185	0.181	2.156	2.688
			SER1 I_{calc} :	6	38	69	10	80	130
SER2 ν (cm^{-1})	SER2 I_{exp}	SER2 I_{calc}							
3610	0.269	44	0.217	0.356	0.356	0.337	0.227	0.295	
2885	0.294	39	0.268	0.342	0.438	0.416	0.279	0.364	
1788	2.180	324	0.239	0.306	0.391	0.372	0.250	0.325	
1608	0.327	40	0.291	0.371	0.476	0.451	0.303	0.395	
1073	0.618	68	0.323	0.413	0.529	0.502	0.337	0.440	
973	0.334	82	0.145	0.185	0.237	0.225	0.151	0.197	
914	0.400	86	0.165	0.211	0.270	0.257	0.172	0.225	
			$K_r = 0.309 \pm 0.099$						
			$K_r[\text{SER3/SER1}]$						
			SER1 ν (cm^{-1}):	3344	1646	1399	1265	1136	1105
			SER1 I_{exp} :	0.169	0.836	1.185	0.181	2.156	2.688
			SER1 I_{calc} :	6	38	69	10	80	130
SER3 ν (cm^{-1})	SER3 I_{exp}	SER3 I_{calc}							
3516	0.164	138	0.042	0.054	0.069	0.065	0.044	0.057	
1624	0.040	41	0.034	0.044	0.056	0.053	0.036	0.047	
592	0.08	87	0.034	0.044	0.056	0.054	0.036	0.047	
			$K_r = 0.049 \pm 0.010$						

scaling of force constants yields better results than the scaling of the frequencies. Scaling of frequencies in the past resulted usually in a frequency inaccuracy of about 10 cm^{-1} for DFT-(B3LYP)/6-31++G** calculations.^{15,28}

Conclusions

In this study, we combined theoretical DFT(B3LYP)/6-31++G** calculations with experimental matrix FT-IR results to demonstrate the presence of four different conformers of serine. The different kinds of intramolecular H-bonds allow to distinguish between these different conformers. We evaluated that all four low energy conformers, SER1, SER2, SER3, and SER4, are present in the low-temperature Ar matrix. Almost all bands of SER1, SER2, and SER3 could be identified in the experimental spectrum, while for SER4 only the most intensive vibrational modes could be observed. Applying the optimal scaling factors for scaling the force constants, which we derived for amino acids, results in a mean frequency deviation of only 5.6 cm^{-1} .

From the free energy difference between the different conformations, a theoretical rotamerization constant can be determined. For the equilibrium SER2/SER1, a value of 0.55 is calculated, and for SER3/SER1, K_r was found to be 0.22. At the same time, experimental rotamerization constants for the two equilibria were derived from the experimental and theoretical intensities. The values are 0.31 and 0.05, respectively. The small disagreement between the theoretical and experimental rotamerization constants is due to the presence of a strong intramolecular hydrogen bond in the conformers SER2 and SER3.

Acknowledgment. B.L. acknowledges financial support from the Institute for the Promotion of Innovation through Science and Technology in Flanders (IWT-Vlaanderen). R.R. thanks the Flemish Fund for Scientific Research (F.W.O.-Vlaanderen) for the Postdoctoral Fellowship.

References and Notes

- (1) Luscombe, N. M.; Laskowski, R. A.; Thornton, J. M. *Nucleic Acids Res.* **2001**, 29 (13), 2860.

- (2) Snyder, L. E.; Hollis, J. M.; Suenram, R. D.; Lovas, F. J.; Brown, L. W.; Buhl, D. *Astrophys. J.* **1983**, 268, 123.
- (3) Ladik, J. J. *THEOCHEM* **2004**, 673, 59.
- (4) <http://www.anyvitamins.com/serine-info.htm>.
- (5) Van Alsenoy, C.; Scarsdale, J. N.; Sellers, H. L.; Schäfer, L. *Chem. Phys. Lett.* **1981**, 80 (1), 124.
- (6) Van Alsenoy, C.; Kulp, S.; Siam, K.; Klimkowski, J.; Ewbank, J. D.; Schäfer, L. *THEOCHEM* **1988**, 181 (1–2), 169.
- (7) Tarakeshwar, P.; Manogram, S. *THEOCHEM* **1994**, 305, 205.
- (8) Gronert, S.; O'Hair, R. A. J. *J. Am. Chem. Soc.* **1995**, 117, 2071.
- (9) Tortonda, F. R.; Silla, E.; Tunon, I.; Rinaldi, D.; Ruiz-Lopez, M. F. *Theor. Chem. Acc.* **2000**, 104, 89.
- (10) Noguera, M.; Rodriguez-Santiago, L.; Sodupe, M.; Bertran, J. J. *Mol. Struct.* **2001**, 537, 307.
- (11) Stepanian, S. G.; Reva, I. D.; Radchenko, E. D.; Rosado, M. T. S.; Duarte, M. L. T. S.; Fausto, R.; Adamowicz, L. *J. Phys. Chem. A* **1998**, 102, 1041.
- (12) Stepanian, S. G.; Reva, I. D.; Radchenko, E. D.; Adamowicz, L. J. *Phys. Chem. A* **1998**, 102, 4623.
- (13) Stepanian, S. G.; Reva, I. D.; Radchenko, E. D.; Adamowicz, L. J. *Phys. Chem. A* **1999**, 103, 4404.
- (14) Stepanian, S. G.; Reva, I. D.; Radchenko, E. D.; Adamowicz, L. J. *Phys. Chem. A* **2001**, 105, 10664.
- (15) Lambie, B.; Ramaekers, R.; Maes, G. *Spectrochim. Acta, Part A* **2003**, 59, 1387.
- (16) Becke, A. D. *J. Chem. Phys.* **1993**, 98, 564.
- (17) Lee, C.; Yang, W.; Parr, R. G. *Phys. Rev. B* **1988**, 37, 785.
- (18) Hobza, P.; Spöner, J.; Reschel, T. *J. Comput. Chem.* **1995**, 1611, 1315.
- (19) *PQS Ab Initio Program Package*, version 2.5; Parallel Quantum Solutions: Fayetteville, AR, 2002.
- (20) *SQM*, version 1.0; Parallel Quantum Solutions: Fayetteville, AR, 2002.
- (21) Baker, J.; Jarzecki, A. A.; Pulay, P. *J. Phys. Chem. A* **1998**, 102, 1412.
- (22) Maes, G. *Bull. Soc. Chim. Belg.* **1981**, 90, 1093.
- (23) Graindourze, M.; Smets, J.; Zeegers-Huyskens, T.; Maes, G. *J. Mol. Struct.* **1990**, 222, 465.
- (24) Ramaekers, R.; Pajak, J.; Lambie, B.; Maes, G. *J. Chem. Phys.* **2004**, 120 (9), 4182.
- (25) Lapinski, L.; Fulara, J.; Nowak, M. J. *Spectrochim. Acta, Part A* **1990**, 46, 61.
- (26) Lapinski, L.; Fulara, J.; Czerminsky, R.; Nowak, M. J. *Spectrochim. Acta, Part A* **1990**, 46, 1087.
- (27) Nowak, M. J.; Lapinski, L.; Fulara, J.; Les, A.; Adamowicz, L. *J. Phys. Chem.* **1992**, 96, 1562.
- (28) Ramaekers, R.; Dehaen, W.; Adamowicz, L.; Maes, G. *J. Phys. Chem. A* **2003**, 107, 1710.